Hole transport and valence-band dispersion law in a HgTe quantum well with a normal energy spectrum

G. M. Minkov,[1,2] A. V. Germanenko,[2] O. E. Rut,[2] A. A. Sherstobitov,[1,2] S. A. Dvoretski,[3] and N. N. Mikhailov[3]

[1]*Institute of Metal Physics RAS, 620990 Ekaterinburg, Russia*

[2]*Institute of Natural Sciences, Ural Federal University, 620000 Ekaterinburg, Russia*

[3]*Institute of Semiconductor Physics RAS, 630090 Novosibirsk, Russia*

(Received 26 February 2014; revised manuscript received 10 April 2014; published 24 April 2014)

The results of an experimental study of the energy spectrum of a valence band in a HgTe quantum well of width $d < 6.3$ nm with normal spectrum in the presence of a strong spin-orbit splitting are reported. The analysis of the temperature, magnetic field, and gate voltage dependences of the Shubnikov–de Haas oscillations allows us to restore the energy spectrum of the two valence-band branches, which are split by the spin-orbit interaction. Comparison with a theoretical calculation shows that a six-band kP theory well describes all the experimental data in the vicinity of the top of the valence band.

DOI: 10.1103/PhysRevB.89.165311 PACS number(s): 73.40.Lq, 73.21.Fg, 73.63.Hs

I. INTRODUCTION

Peculiarities of the energy spectrum of the spatially confined gapless semiconductors (HgTe, HgSe) results in unique transport, optical, and other properties of the carriers in structures with quantum wells based on such materials. Theoretically, the energy spectrum of confined gapless semiconductors has been intensively studied since 1982 [1–4]. It was shown that a Dirac-like spectrum linear in quasimomentum should be realized at some critical width of the HgTe quantum well, $d = d_c \simeq 6.3$ nm in CdTe/HgTe/CdTe heterostructures [5]. Just these structures attract especial attention from both theoreticians and experimentalists.

When the quantum well width is not equal to d_c, the energy spectrum is more complicated. Calculations show that the quasimomentum dependence of the carrier energy $E(k)$ for the conduction band is simple enough both for wide ($d > d_c$) quantum wells with inverse subband ordering and for narrow ($d < d_c$) wells with a normal spectrum. The dispersion for electrons is analogous to the spectrum of the conduction band of the usual narrow-gap semiconductors. It is close to parabolic in shape at small quasimomentum (this area shrinks to zero when the well width tends to d_c), crosses over to linear as k increases, and becomes parabolic again with further increase of k. The spectrum of the valence band is much more complicated. Even at d close to d_c it is similar to the spectrum of the conduction band only within a narrow range of energy near the top of the valence band. In wider quantum wells, $d > d_c$, the spectra of valence and conduction bands differ greatly. At $d > 10$–12 nm, the valence-band dispersion becomes nonmonotonic, namely, an electronlike section appears at $k \simeq 0$. In narrower quantum wells, $d < d_c$, the dispersion of the valence band is nontrivial as well. Together with the main maximum at $k = 0$, secondary maxima in the dependence $E(k)$ arise at large k as theory predicts.

The experimental study of magnetotransport and the energy spectrum and their dependence on the well width became possible only 10–15 years ago. This is primarily due to the impressive progress in technology [6,7]. Although the experimental studies are mainly focused on the investigation of the quantum and spin Hall effects [5,8–11], there is a number of papers [12–20] where the spectrum of carriers is studied. However, only four of them, Refs. [13–16], are devoted to the valence band. One of the key results of the papers is that the dependence $E(k)$ in structures with $d > 10$–15 nm is really nonmonotonic and the electronlike section really appears at $k \simeq 0$. This result is in qualitative agreement with the calculated ones; however, there are very significant quantitative discrepancies with theoretical predictions [16].

The energy spectrum of the valence band in the structures with a normal spectrum ($d < d_c$) was experimentally studied only in Ref. [14]. The measurements were taken at fixed hole density $p = 3 \times 10^{11}$ cm^{-2}; therefore the interpretation of the data does not seem very reliable.

In this paper, we report the results of an experimental study of the hole transport in a HgTe quantum well with a normal energy spectrum. The measurements were performed over a wide range of hole densities. Analysis of the experimental data allows us to reconstruct the energy spectrum of the $H1$ hole subband, which has been shown to be in good agreement with the results of the kP theory.

II. EXPERIMENT

Our HgTe quantum wells were realized on the basis of a HgTe/$Hg_{1-x}Cd_xTe$ ($x = 0.55$–0.65) heterostructure grown by molecular beam epitaxy (MBE) on a GaAs substrate with (013) surface orientation [7]. A sketch of the structures investigated is shown in the inset of Fig. 1(a). The nominal width of the quantum well was $d = 5.8$, 5.6, and 5.0 nm in the structures H724, H1122, and H1310, respectively. The results for all the structures are similar and we will discuss the results that were obtained in the structure H724 with the highest Hall mobility. The samples were mesa etched into standard Hall bars of 0.5 mm width and with a distance between the potential probes of 0.5 mm. To change and control the hole density (p) in the quantum well, field-effect transistors were fabricated with Parylene as the insulator and aluminum as the gate electrode. The measurements were performed at temperature of 1.3–4.2 K in magnetic fields B up to 7 T.

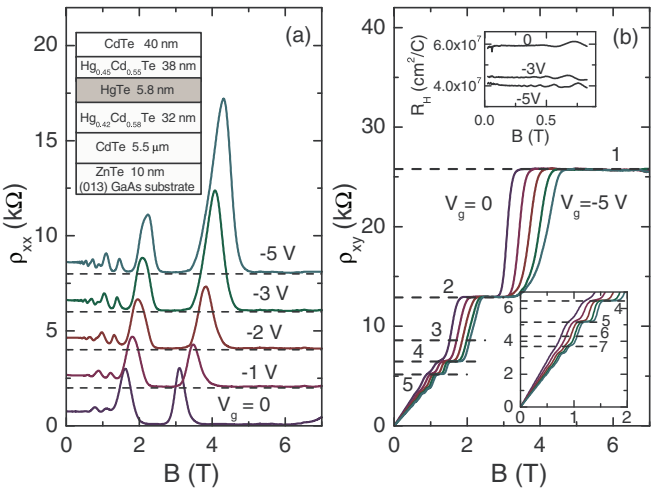

FIG. 1. (Color online) The magnetic field dependences of ρ_{xx} (a) and ρ_{xy} (b) measured for the different gate voltages. The inset in (a) shows a sketch of the structure H724. The upper inset in (b) demonstrates the magnetic field dependence of the Hall coefficient at low magnetic field; the lower inset shows ρ_{xy} at $B < 2$ T.

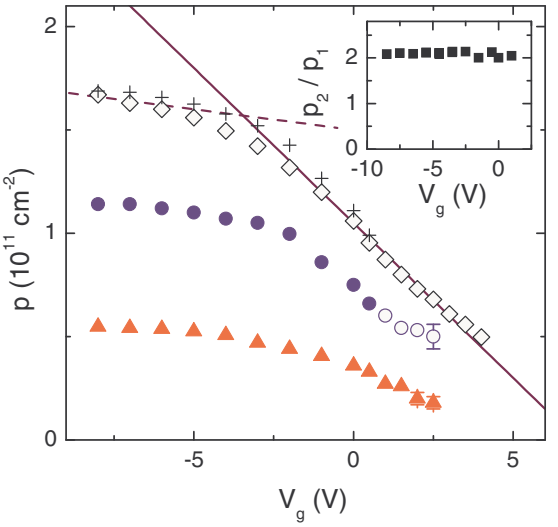

FIG. 2. (Color online) The gate voltage dependence of the Hall density $p_{\rm H} = 1/[eR_{\rm H}(0.1\,{\rm T})]$ (diamonds) and densities p_1 and p_2 (circles and triangles, respectively) found from the SdH oscillations (see text). The open circles are p_2 found as $p_{\rm H} - p_1$. The crosses are the sum $p_1 + p_2 = p_{\rm tot}$. The solid and dashed straight lines are drawn with the slopes -1.5×10^{10} cm^{-2} V^{-1} and -0.2×10^{10} cm^{-2} V^{-1}, respectively. The inset shows the V_g dependence of the ratio p_2/p_1.

III. RESULTS AND DISCUSSION

An overview of the magnetic field dependences of the longitudinal and transverse resistivity (ρ_{xx} and ρ_{xy}, respectively) for different gate voltages (V_g) is presented in Fig. 1. Well-defined quantum Hall plateaus in ρ_{xy} and minima in ρ_{xx} are evident. It should be noted that the plateaus with the numbers 3 and 6 [see the lower inset in Fig. 1(b)] are not observed. This point will be discussed later. As clearly seen from the upper inset in Fig. 1(b), the Hall coefficient $R_{\rm H} = \rho_{xy}/B$ is almost independent of the magnetic field in the low-field domain $B \simeq 0.01$–0.2 T, where the Shubnikov–de Haas (SdH) oscillations are not observed yet. One can therefore assume that the density of holes can be obtained as $p_{\rm H} = 1/[eR_{\rm H}(0.1\,{\rm T})]$. The gate voltage dependence of the hole Hall density so obtained is presented in Fig. 2 by diamonds. One can see that $p_{\rm H}$ linearly changes with V_g with a slope $|dp_{\rm H}/dV_g|$ of about 1.5×10^{10} cm^{-2} V^{-1} at $-3.5 < V_g < 4$ V, where the hole density is less than 1.5×10^{11} cm^{-2}. At $V_g \lesssim -3.5$ V, the slope becomes much less; $|dp_{\rm H}/dV_g| \simeq 0.2 \times 10^{10}$ cm^{-2} V^{-1}. Note that the capacitance C between the gate electrode and the two-dimensional channel in this sample is constant over the whole gate voltage range so that the value of $C/e = (1.4 \pm 0.15) \times 10^{10}$ cm^{-2} V^{-1} is almost the same as $|dp_{\rm H}/dV_g| = 1.5 \times 10^{10}$ cm^{-2} V^{-1} observed at $-3.5 < V_g < 4$ V. Possible reasons for the $|dp_{\rm H}/dV_g|$ decrease evident at $V_g < -3$ V are considered at the end of this section. The Hall mobility $\mu_{\rm H} = \sigma R_{\rm H}(0.1\,{\rm T})$, where σ stands for the conductivity at $B = 0$, increases with increase of $p_{\rm H}$, achieves the maximal value of about 8×10^4 cm^2/(V s) at $p_{\rm H} = 1.3 \times 10^{11}$ cm^{-2}, and demonstrates a slight decrease with further $p_{\rm H}$ increase (not shown).

Another way to determine the hole density is by analysis of the SdH oscillations. The experimental SdH oscillations of ρ_{xx} are shown for several gate voltages in Fig. 3(a), while the corresponding Fourier spectra are presented in Fig. 3(b). Two

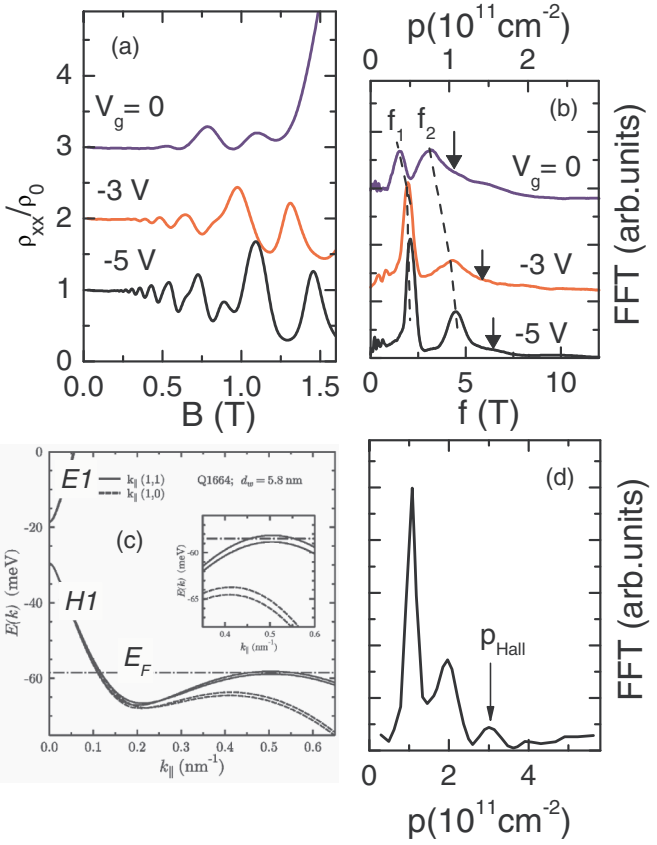

FIG. 3. (Color online) The SdH oscillations for some gate voltages (a) and their Fourier spectra (b); the calculated energy spectrum (c) and the Fourier spectrum of the SdH oscillations (d) from Ref. [14]. Arrows in (b) correspond to $p_{\rm H}$. The scale of the top axis in (b) is associated with that of the bottom axis via $p = ef/(2\pi\hbar)$.

maxima with the frequencies f_1 and f_2, which are shifted with the gate voltage, can be easily detected in the Fourier spectra.[1] It is noteworthy that the ratio of the frequencies f_2/f_1 is close to 2. So the Fourier spectra are analogous to those in the case when the spin splitting of the Landau levels manifests itself with magnetic field increase. In such a situation the carrier density should be determined as $p_{\mathrm{SdH}} = ef_1/(\pi\hbar)$. If this is true in our case, we obtain a p_{SdH} which is significantly less than the hole density p_{H} obtained from the Hall effect. For example, inspection of Fig. 3(b) reveals $f_1 \simeq 2$ T for $V_g = -3$ V which yields $p_{\mathrm{SdH}} \simeq 0.95 \times 10^{11}$ cm^{-2}, whereas the Hall effect for this gate voltage gives a much larger value, $p_{\mathrm{H}} \simeq 1.4 \times 10^{11}$ cm^{-2} (see Fig. 2).

Before interpreting our data let us recall that very similar results were obtained in Ref. [14] for a HgTe quantum well of the same nominal width but with somewhat larger Hall density, $p_{\mathrm{H}} = 3 \times 10^{11}$ cm^{-2} [see Fig. 3(d)]. As seen from the figure two maxima in the Fourier spectrum with a ratio of frequencies of about 2 were observed also in that paper. Thus the hole density found from the SdH oscillations turns out to be less than the Hall density. The authors of Ref. [14] attributed this discrepancy to the peculiarity of the valence-band energy spectrum. The energy spectrum calculated for the actual energy range in Ref. [14] is presented in Fig. 3(c). As seen there are additional maxima in the dispersion of the valence band $H1$ in the (1,1) direction at $k_\parallel \simeq 0.5$ nm^{-1}. These maxima are situated 28 meV below the main maximum at $k_\parallel = 0$. In accordance with the calculation, the authors of Ref. [14] reasoned that the experimental peak corresponding to $p = 1 \times 10^{11}$ cm^{-2} is two merged peaks centered at $p = 1.01 \times 10^{11}$ cm^{-2} and $p = 0.97 \times 10^{11}$ cm^{-2}, which originate from the spin-orbit-split $H1-$ and $H1+$ subbands at $k_\parallel \approx 0$. The peak at $p = 1.95 \times 10^{11}$ cm^{-2} corresponds to the sum of the hole densities in these subbands. So the hole density p_{SdH} found from the SdH oscillations is about 2×10^{11} cm^{-2} according to the interpretation given in Ref. [14]. The difference between the Hall density $p_{\mathrm{Hall}} = 3 \times 10^{11}$ cm^{-2} [see Fig. 3(d)] and SdH density $p_{\mathrm{SdH}} = 2 \times 10^{11}$ cm^{-2}, which is about 1×10^{11} cm^{-2}, has been attributed to the holes in the four secondary maxima at $k_\parallel = 0.5$ nm^{-1}. According to the authors of [14] "A peak in the Fourier spectrum due to these holes could be expected; however, this should occur at a very low frequency corresponding to $p = 0.24 \times 10^{10}$ cm^{-2} and is therefore not observed". It is clear in the framework of this model that the reduction of the total hole density to 2×10^{11} cm^{-2} and below should lead to the disappearance of the contribution of the carriers from the secondary maxima and, thus, should lead to agreement between the Hall and SdH densities. Unfortunately, the structure studied in Ref. [14] was ungated; therefore the authors could not control the density of the carriers to check this interpretation. So the results of Ref. [14] do not seem very conclusive.

In the structures investigated in the present paper, the difference between the density found from the SdH oscillations within the above model and the density found from the Hall effect is observed over the whole gate voltage range, where the hole density changes from 0.6×10^{11} cm^{-2} to 1.7×10^{11} cm^{-2}. Thus, this interpretation does not correspond to our case.

The only model that describes our results is as follows. As in Ref. [14], we suppose that the subband of spatial quantization $H1$ is split by spin-orbit interaction into two subbands, $H1+$ and $H1-$, due to asymmetry of the quantum well. But in contrast to Ref. [14], we believe that the spin-orbit splitting is so large that the two maxima evident in our Fourier spectra originate just from these $H1+$ and $H1-$ subbands. Under this assumption the hole densities in the split subbands should be found as $p_{1,2} = ef_{1,2}/(2\pi\hbar)$, where the indices 1 and 2 correspond to $H1+$ and $H1-$, respectively. The factor of 2 in the denominator is due to the absence of "spin" degeneracy of the split subbands. The total density in this case is the sum of p_1 and p_2; $p_{\mathrm{tot}} = p_1 + p_2$. The results of such a data treatment are presented in Fig. 2 within the gate voltage range from -8.5 to $+0.5$ V, where we were able to determine reliably the frequencies for both peaks in the Fourier spectra. One can see that the values of p_{tot} coincide with p_{H}, to within experimental error. At $V_g > 0.5$ V, we could determine the frequency of only the low-frequency Fourier component resulting from the quantization of the $H1+$ subband. In this case the hole density in the second subband, $H1-$, was found as $p_2 = p_{\mathrm{H}} - p_1$ (depicted by the open circles in Fig. 2). As seen, these data match the data obtained directly from the Fourier spectra at $V_g < 0.5$ V well.

The inset in Fig. 2 shows that the ratio of the hole densities in spin-orbit-split subbands is essentially independent of the gate voltage and is about 2 over the whole gate voltage range. Such a large ratio is evidence of giant spin-orbit splitting.[2]

At first sight the large spin-orbit splitting of the energy spectrum in the nominally almost symmetrical structure [see the inset in Fig. 1(a)] seems very surprising. However, one must take into account the peculiarity of the MBE growth process of the $Hg_{1-x}Cd_xTe$/HgTe heterostructures. There is an overpressure of tellurium during the growth process, and therefore mercury vacancies are present in the structure at the end of growth. They are the acceptors in $Hg_{1-x}Cd_xTe$, and therefore the major carriers in the quantum well should be the holes. Nevertheless, the heterostructures as a rule demonstrate n-type conductivity after evacuation from the growth chamber. It is believed that this is because mercury overpressure remains in the chamber after completion of growth. During the cooling, the mercury vacancies are annealed. When the cooling time is small, the upper barrier is converted to n type, while the lower

[1]Note that in order to find the parameters of the energy spectrum from the SdH oscillations one should make the Fourier analysis at low enough magnetic field where the oscillations of the Fermi energy with the magnetic field can be neglected, i.e., where $\delta\rho_{xx}/\rho_{xx} \ll 1$.

[2]It might be expected that the existence of two types of carriers corresponding to the two spin-orbit-split subbands should reveal itself in the magnetic field dependences of the Hall coefficient and longitudinal resistance. However, it is easy to check that for such a ratio between the densities and with a ratio between the mobilities of about 1.5–2, the change of R_{H} and ρ_{xx} in classical magnetic fields should be about 4%–7% only. In fact, changes of R_{H} and ρ_{xx} with magnetic field of about 3%–5% are observed; however, it is impossible to find four parameters unambiguously from these dependencies.

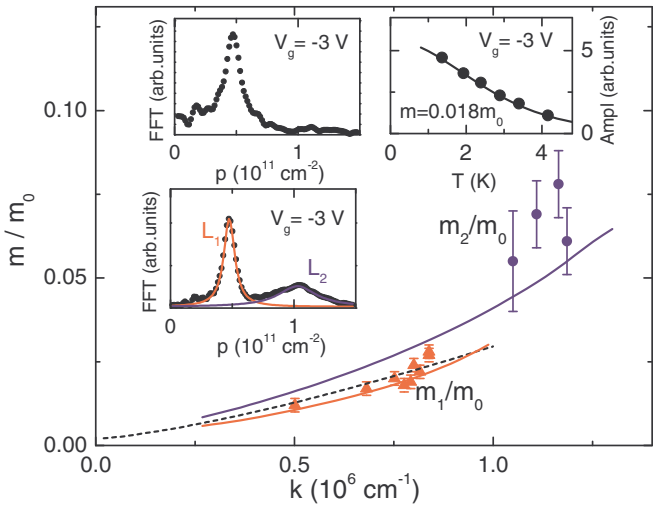

FIG. 4. (Color online) The values of the hole effective mass in the subbands $H1+$ (triangles) and $H1-$ (circles) found at different quasimomenta $k_{1,2} = \sqrt{p_{1,2}/4\pi}$. The dotted line is the interpolation dependence for the m_1 vs k data. The solid lines are the result of the theoretical calculation (see text). The left upper and lower insets show the Fourier spectra of the oscillations of ρ_{xx} taken at $V_g = -3$ V within the magnetic field ranges 0.1–0.4 and 0.1–1.1 T, respectively. The lines in the lower inset are the best fit with two Lorentzians. The right inset is the temperature dependence of the oscillation amplitude at $B = 0.3$ T (symbols) and the result of the best fit by the Lifshits-Kosevich formula [22] with $m = 0.018m_0$ (line).

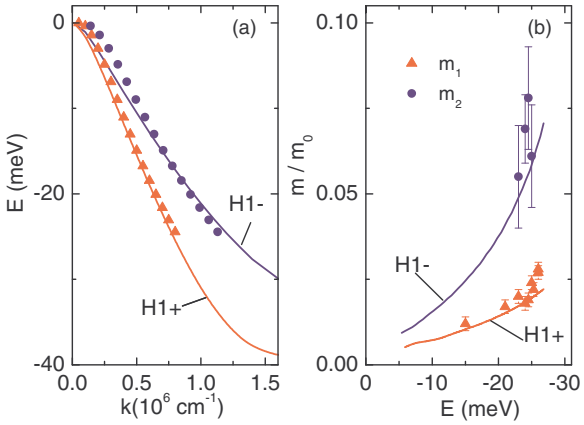

FIG. 5. (Color online) The energy dispersion (a) and the effective mass plotted against the energy (b) for the $H1+$ and $H1-$ hole subbands. Symbols are taken from the experimental data; the solid lines are the results of a theoretical calculation taking into account the electric field in the well.

barrier can remain of p type. In this case, the quantum well is brought into the p-n junction and the strong electric field of the junction should lead to spin-orbit splitting due to the Rashba effect [21].

Thus, the analysis of the gate voltage dependences of the Hall density and SdH oscillations shows that we are dealing with structures whose valence band is strongly split due to spin-orbit interaction. Knowing this, we are in position to study the spectrum in more detail.

In order to do this we have determined the hole effective mass by analyzing the temperature dependence of the amplitude of the SdH oscillations. As seen from the left upper inset in Fig. 4, the main contribution to the SdH oscillations at low enough magnetic field comes from the one spin-orbit-split subband $H1+$, which gives the lower frequency to the Fourier spectrum. Thus, the effective mass m_1 found from the SdH oscillations within this magnetic field range will correspond to the mass in the $H1+$ subband. As an example, the temperature dependence of the amplitude of SdH oscillations at $B = 0.3$ T measured at $V_g = -3$ V is shown in the right inset in Fig. 4. A fit of this dependence by the Lifshits-Kosevich formula [22] (shown by the line) gives $m_1 = (0.018 \pm 0.003)m_0$. Such an analysis performed for the different gate voltages gives the quasimomentum dependence of the effective mass m_1, which is plotted in Fig. 4 by the triangles. One can see that m_1 increases with k significantly.

The experimental determination of the effective mass in the second subband $H1-$ is much more difficult. With this aim, we have decomposed the Fourier spectra for every temperature by fitting them by two Lorentzians L_1 and L_2 (see the left lower inset in Fig. 4). Then, after inverse Fourier transformation of L_2 we obtained oscillations coming solely from the $H1-$ subband. Treating the temperature dependence of the amplitude of these oscillations we have found the effective mass m_2. The results are shown in Fig. 4 by the circles.

Knowing the m vs k dependence and assuming an isotropic energy spectrum one can restore the dispersion $E(k)$: $E(k) = \int_0^k k/m(k)dk$. Because m_1 is measured within a wider interval of k, we first obtained $E(k)$ for the $H1+$ subband. Using the interpoled dependence $m(k)$ shown in Fig. 4 by the dotted curve, we have obtained the dependence $E(k)$, which is depicted in Fig. 5(a) by the triangles. To restore the dispersion of the $H1-$ subband we use the fact that the ratio of the hole densities in the $H1-$ and $H1+$ subbands is about 2 over the whole gate voltage range (see the inset in Fig. 2). So the dispersion of the $H1-$ subband has been obtained from the $H1+$ dispersion by scaling with the factor $\sqrt{2}$ in the k direction. The value of the spin-orbit splitting is really gigantic: for example, it is about 8 meV at the Fermi energy 20 meV, i.e., approximately 40%, Now, when we have restored the E vs k dependence we can find the energy dependence of the effective masses [see Fig. 5(b)]. It is seen that m_1 increases strongly with the energy and m_2 is 2–3 times larger than m_1.

To compare the experimental results with theory, we have calculated the energy spectrum within the framework of the six-band kP model taking into account the lattice mismatch between the $Hg_{1-x}Cd_xTe$ layers forming the quantum well and the CdTe buffer layer. The calculations were performed within the framework of the isotropic approximation using the direct integration technique as described in Ref. [23]. The electrostatic potential has been obtained self-consistently from the simultaneous solution of the Poisson and Schrödinger equations. The donor and acceptor densities in the upper and lower barriers, respectively, were supposed to be equal to 3×10^{17} cm^{-3}. The other parameters were the same as in Refs. [24,25].

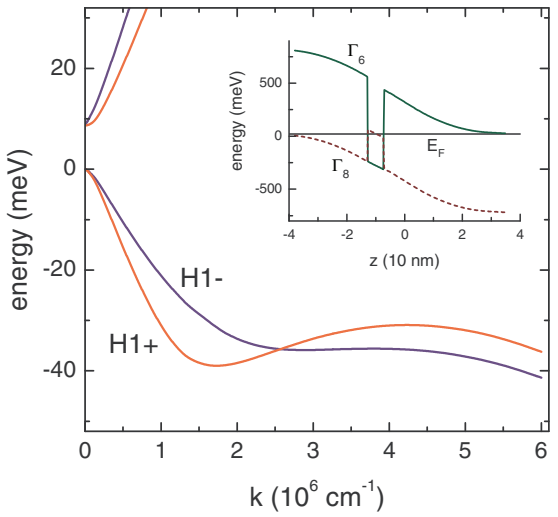

FIG. 6. (Color online) The results of self-consistent calculation of the energy spectrum of the conduction and valence bands. The inset shows the energy diagram of the structure on the assumption that acceptor and donor densities in the lower and upper barriers, respectively, are 3×10^{17} cm^{-3}.

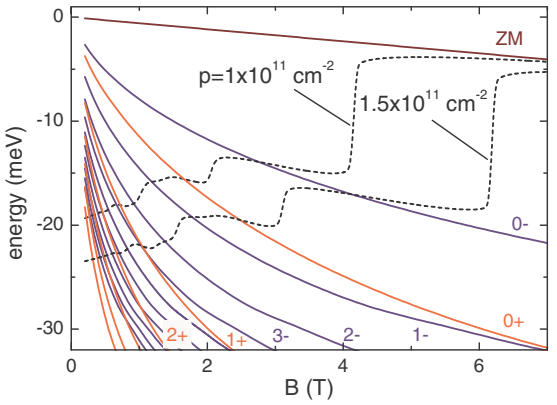

FIG. 7. (Color online) The energy of the Landau levels as a function of magnetic field calculated within the semiclassical approximation. The dotted lines represent the Fermi level for two hole densities calculated with a Landau level broadening of 1 meV. The Landau levels are labeled with the quantum numbers N; the indices $+$ and $-$ indicate from which subband, $H1+$ or $H1-$, the levels originate. The zero-mode Landau level is labeled as ZM.

The calculated energy diagram and the dispersion law $E(k)$ for the heterostructure H724 are shown within a wide k range in Fig. 6. As clearly seen, the energy spectrum of the valence and conduction bands is strongly split due to the Rashba effect. A peculiarity of the spectrum is that the positions of the branches $H1+$ and $H1-$ are interchanged at $k \simeq 2.5 \times 10^6$ cm^{-1}.

To correlate theoretical and experimental results, we have depicted the calculated dependences $m(k)$, $E(k)$, and $m(E)$ on the same figures in which the experimental data are presented [see Figs. 4, 5(a), and 5(b), respectively]. It is evident that in the range where the experimental data were obtained, they are in good agreement with the theoretical curves, suggesting the adequacy of the model used.

Let us now turn to the peculiarity of the quantum Hall effect mentioned in the beginning of this section and evident as the absence of the quantum Hall plateaus with the numbers 3 and 6 [see Fig. 1(b)]. Interestingly, the absence of the same plateaus was also observed but not commented on and discussed in Ref. [14] (see Fig. 7 in that paper). To understand this feature, one should calculate the Landau levels. It can be done in principle with the use of one of the techniques presented in the literature [25,26]. However, a qualitative explanation can already be obtained within the much simpler semiclassical quantization approximation. The energy of the Nth Landau level, E_N, in the magnetic field B can be obtained in this case by substitution of $(2N+1)/l^2$ instead of k^2 in the dependence $E(k)$, where $l = \sqrt{\hbar/eB}$ is the magnetic length. Moreover, it must be taken into account that there is an additional zero-mode Landau level for such a spectrum, whose position is almost independent of the magnetic field [16,25–27]. In Fig. 7, we have depicted a fan-chart diagram calculated in this manner for the spectrum shown in Fig. 5(a). The dotted lines in this figure are the Fermi levels calculated with Landau level broadening of 1 meV for the two hole densities $p = 1 \times 10^{11}$ cm^{-2} and 1.5×10^{11} cm^{-2}. One can see that the energy distances between the levels $1-$ and $0+$ and the levels $3-$ and $2+$ near the Fermi level within this hole density range are less noticeable than those between the other levels. Therefore, the localized states between these Landau levels are absent so the ρ_{xy} plateaus with the numbers 3 and 6 have not been observed.

Another feature mentioned above is that the p vs V_g dependence is flattened at $V_g \simeq -3.5$ V when the density reaches the value 1.5×10^{11} cm^{-2} as the gate voltage is lowered (Fig. 2). There are two possibilities to explain this behavior. The first one results from the peculiarity of the energy spectrum. It is easy to estimate from Fig. 5(a) that the Fermi level at $p = 1.5 \times 10^{11}$ cm^{-2} lies at an energy of about -25 meV. As seen from Fig. 6, this value is close to the energy of the secondary maxima in the dependence $E(k)$, located at $k \simeq 4 \times 10^6$ cm^{-1}. Because of the large effective mass in these maxima the sinking speed of the Fermi level decreases strongly when these states are being occupied at $V_g < -3.5$ V. In the presence of potential fluctuations, these states can be localized and, hence, they will not contribute to the conductivity. In this case, the Hall density will correspond to the hole density in the main maximum, while the total charge of carriers in the well will be determined by the density in all the maxima. In favor of this conclusion is the fact that the flattening of the dependence $p(V_g)$ is observed in all three structures under study.

The second possibility to explain the feature under discussion is the existence of localized states in the lower barrier which start to be occupied as the gate voltage decreases just at $V_g \simeq -3.5$ V. This should also result in the saturating behavior of the hole density at $V_g \lesssim -3.5$ V. We cannot exclude this mechanism at the moment.

IV. CONCLUSION

We have studied the transport phenomena in narrow ($d < d_c$) HgTe-based quantum wells of p-type conductivity with a normal energy spectrum. In analyzing the data we have reconstructed the dispersion law near the top of the valence band at $k \lesssim 10^6$ cm^{-1}. It has been shown that the hole energy

spectrum is strongly split by spin-orbit interaction, so that the ratio of the holes in the split subbands is approximately equal to 2. It has been shown that the energy spectrum is strongly nonparabolic, namely, the hole effective masses significantly increase with energy increase. These results are well described in the framework of the kP model if one supposes that the lower barrier remains of p type, while the upper one is converted to n type after growth stops, so that the quantum well is located in the strong electric field of a p-n junction.

It is noteworthy that the above conclusion about the adequacy of the kP model for description of the hole energy spectrum is opposite to the conclusion made in our previous paper [16] on wide ($d > d_c$) HgTe quantum wells with an inverted spectrum. It was there shown that the valence-band spectrum is electronlike near $k = 0$ so the top of the band is located at $k \neq 0$. The key result of the paper, however, was that the experimental and calculated hole spectra, though in qualitative agreement, were strongly different quantitatively within the whole range of experimentally accessible quasimomentum values, $k \lesssim 1.7 \times 10^6$ cm^{-1}.

One of the possible reasons why the theory works well in the narrow HgTe quantum wells and does not explain the data in wide wells is the following. The top of the valence band is formed from the different subbands of spatial quantization in narrow and wide quantum wells. The top is the $H1$ subband in the first case and the $H2$ subband in the second one. Thus it turns out that the standard kP model describing the dispersion of the $H1$ subband fails to describe the spectrum of the $H2$ subband for whatever reason. The other possible reason concerns the band gap. In the quantum wells investigated in the present paper, the valence and conduction bands are separated by the gap. The systems investigated in Ref. [16] are semimetallic, and therefore electrons and holes can coexist in that case. The workability of the single-particle approximation in such a situation can be really questionable and a many-particle approach could be more adequate. In any case, this problem requires further investigation.

ACKNOWLEDGMENTS

We thank A. Ya. Aleshkin and M. S. Zholudev for helpful discussions. Partial financial support from the RFBR (Grants No. 12-02-00098 and No. 13-02-00322) and from the Program of the RAS Presidium (Project No. 12-P-2-1051) is gratefully acknowledged.

[1] M. I. D'yakonov and A. Khaetskii, Zh. Eksp. Teor. Fiz. **82**, 1584 (1982) [Sov. Phys. JETP **55**, 917 (1982)].
[2] Y. R. Lin-Liu and L. J. Sham, Phys. Rev. B **32**, 5561 (1985).
[3] M. V. Kisin and V. I. Petrosyan, Fis. Tekh. Poluprovodn. **22**, 829 (1988) [Sov. Phys. Semicond. **22**, 523 (1988)].
[4] L. G. Gerchikov and A. Subashiev, Phys. Status Solidi (b) **160**, 443 (1990).
[5] B. A. Bernevig, T. L. Hughes, and S.-C. Zhang, Science **314**, 1757 (2006).
[6] F. Goschenhofer, J. Gerschutz, A. Pfeuffer-Jeschke, R. Hellmig, C. R. Becker, and G. Landwehr, J. Electron. Mater. **27**, 532 (1998).
[7] N. N. Mikhailov, R. N. Smirnov, S. A. Dvoretsky, Y. G. Sidorov, V. A. Shvets, E. V. Spesivtsev, and S. V. Rykhlitski, Int. J. Nanotechnol. **3**, 120 (2006).
[8] M. König, S. Wiedmann, C. Brüne, A. Roth, H. Buhmann, L. W. Molenkamp, X.-L. Qi, and S.-C. Zhang, Science **318**, 766 (2007).
[9] C. Brüne, A. Roth, E. G. Novik, M. Knig, H. Buhmann, E. M. Hankiewicz, W. Hanke, J. Sinova, and L. W. Molenkamp, Nat. Phys. **6**, 448 (2010).
[10] G. M. Gusev, E. B. Olshanetsky, Z. D. Kvon, N. N. Mikhailov, S. A. Dvoretsky, and J. C. Portal, Phys. Rev. Lett. **104**, 166401 (2010).
[11] G. M. Gusev, A. D. Levin, Z. D. Kvon, N. N. Mikhailov, and S. A. Dvoretsky, Phys. Rev. Lett. **110**, 076805 (2013).
[12] A. Pfeuffer-Jeschke, F. Goschenhofer, S. J. Cheng, V. Latussek, J. Gerschütz, C. Becker, G. R. R., and G. Landwehr, Physica B **256-258**, 486 (1998).
[13] G. Landwehr, J. Gerschütz, S. Oehling, A. Pfeuffer-Jeschke, V. Latussek, and C. R. Becker, Physica E **6**, 713 (2000).
[14] K. Ortner, X. C. Zhang, A. Pfeuffer-Jeschke, C. R. Becker, G. Landwehr, and L. W. Molenkamp, Phys. Rev. B **66**, 075322 (2002).
[15] Z. D. Kvon, E. B. Olshanetsky, E. G. Novik, D. A. Kozlov, N. N. Mikhailov, I. O. Parm, and S. A. Dvoretsky, Phys. Rev. B **83**, 193304 (2011).
[16] G. M. Minkov, A. V. Germanenko, O. E. Rut, A. A. Sherstobitov, S. A. Dvoretski, and N. N. Mikhailov, Phys. Rev. B **88**, 155306 (2013).
[17] X. C. Zhang, A. Pfeuffer-Jeschke, K. Ortner, C. R. Becker, and G. Landwehr, Phys. Rev. B **65**, 045324 (2002).
[18] X. C. Zhang, K. Ortner, A. Pfeuffer-Jeschke, C. R. Becker, and G. Landwehr, Phys. Rev. B **69**, 115340 (2004).
[19] G. M. Gusev, Z. D. Kvon, O. A. Shegai, N. N. Mikhailov, S. A. Dvoretsky, and J. C. Portal, Phys. Rev. B **84**, 121302 (2011).
[20] M. V. Yakunin, A. V. Suslov, S. M. Podgornykh, S. A. Dvoretsky, and N. N. Mikhailov, Phys. Rev. B **85**, 245321 (2012).
[21] Y. A. Bychkov and E. I. Rashba, J. Phys. C **17**, 6039 (1984).
[22] I. M. Lifshits and A. M. Kosevich, Zh. Eksp. Teor. Fiz. **29**, 730 (1955) [Sov. Phys. JETP **2**, 636 (1956)].
[23] V. A. Larionova and A. V. Germanenko, Phys. Rev. B **55**, 13062 (1997).
[24] X. C. Zhang, A. Pfeuffer-Jeschke, K. Ortner, V. Hock, H. Buhmann, C. R. Becker, and G. Landwehr, Phys. Rev. B **63**, 245305 (2001).
[25] E. G. Novik, A. Pfeuffer-Jeschke, T. Jungwirth, V. Latussek, C. R. Becker, G. Landwehr, H. Buhmann, and L. W. Molenkamp, Phys. Rev. B **72**, 035321 (2005).
[26] M. S. Zholudev, A. V. Ikonnikov, F. Teppe, M. Orlita, K. V. Maremyanin, K. E. Spirin, V. I. Gavrilenko, W. Knap, S. A. Dvoretskiy, and N. N. Mihailov, Nanoscale Res. Lett. **7**, 534 (2012).
[27] B. Buttner, C. X. Liu, G. Tkachov, E. G. Novik, C. Brune, H. Buhmann, E. M. Hankiewicz, P. Recher, B. Trauzettel, S. C. Zhang, and L. W. Molenkamp, Nat. Phys. **7**, 418 (2011).